Journal Pre-proofs

Transient response to perturbations in flow synthesis of citrate capped gold nanoparticles

Atul H. Bari, Neerja Shukla, Asterios Gavriilidis, Amol A. Kulkarni

PII: S1385-8947(23)02621-9
DOI: https://doi.org/10.1016/j.cej.2023.143890
Reference: CEJ 143890

To appear in: *Chemical Engineering Journal*

Received Date: 28 November 2022
Revised Date: 26 May 2023
Accepted Date: 30 May 2023

Please cite this article as: A.H. Bari, N. Shukla, A. Gavriilidis, A.A. Kulkarni, Transient response to perturbations in flow synthesis of citrate capped gold nanoparticles, *Chemical Engineering Journal* (2023), doi: https://doi.org/10.1016/j.cej.2023.143890

Transient Response to Perturbations in Flow Synthesis of Citrate Capped Gold Nanoparticles

Atul H Bari[1#], Neerja Shukla[1#], Asterios Gavriilidis[3] and Amol A. Kulkarni[1,2,*]

[1]*Chem. Eng. & Proc. Dev. Division, CSIR-National Chemical Laboratory, Pune 411008, India*

[2]*Academy of Scientific & Innovative Research (AcSIR), CSIR-NCL Campus, Pune 411008, India*

[3]*Department of Chemical Engineering, University College London, Torrington Place, London, WC1E 7JE, United Kingdom*

[#]These authors have contributed equally to this paper.

* Corresponding author, (E-mail: aa.kulkarni@ncl.res.in), Phone: +91-20-25902153, Fax: +01-20-25902622

Abstract

This work reports the transient behavior of continuous flow synthesis of gold nanoparticles (Au NPs) when subjected to perturbations in operating conditions using controlled experiments. The intricacies are captured through a detailed mathematical model. Reversed Turkevich protocol was used for synthesis of Au NPs. The synthesis was first studied in batch mode to investigate the reaction kinetics and reproducibility of the process. The optimal set of operating conditions viz., residence time, flow rate, temperature was then used for flow synthesis in a 2 m, 1/16" Polytetrafluoroethylene (PTFE) reactor with micromixer. Reactor clogging was avoided by using segmented flow. Inline UV measurement was used for real time monitoring of the process. Transient experiments were performed by abruptly changing the operating conditions. A mathematical model was found to be accurate in predicting the transient behavior of the exit precursor concentration and the particle size for unsteady state synthesis. Even a small change in process variables for short duration was found to disturb the quality of Au NPs for a significantly longer duration. Of the three operating parameters, the effect of temperature variation was seen to have a prolonged effect where the system remained in unsteady state for long time.

Keywords: Gold nanoparticles, unsteady behavior, continuous flow synthesis, particle size, segmented flow

1. Introduction

Over the past decade research on the size and shape selective synthesis of metal nanoparticles (NPs) has had an increasing impact on materials and surface science related applications. These nanoparticles show a great potential for catalysis as well as for other applications viz. sensing (1), coating, printing (2), diagnostics (3), targeted drug delivery (4), bioimaging etc. In the nanoform, these materials have characteristic features such as optical, electronic, physico-chemical properties, which are different from their bulk form. While a few of these metallic nanoparticles are used at very large scale i.e. few tens of tons every year, several of them are used at very small quantities, i.e. few kg/year. In general, most of these are high value/low volume materials. The conventional synthesis based on bottom up approach for some of these NPs is not easily scalable. The precise dependence of particle nucleation and growth on temperature, concentration of reacting species, proximity of the stabilizing species and the pH in the vicinity of the growing particle play a major role on deciding the particle size distribution (5). These approaches need detailed engineering analysis to translate them into a large scale nanoparticle synthesis process. Since the properties of these NPs are sensitive to their size and shape, minor variations in process conditions can lead to a very different material or even waste. Thus, it is advantageous to monitor the quality of product during manufacturing and change the process parameters accordingly.

Continuous flow synthesis facilitates consistency in the particle size and shape and thereby provides an opportunity to directly interface analytical techniques during synthesis. Also, the continuous flow processes have the potential to address issues of product quality, and process robustness. Recent developments in the field of real time analysis have enabled the development of flow synthesis of NPs with inline monitoring of particle sizes as well as the extent of reaction (6). Such detection systems are able to extract data for the size, shape and chemical composition of NP's on a millisecond timescale. For example, online spectroscopic methods have been used along with flow reactors for NPs synthesis (7-10). Sounart et al. (7) used spatially resolved photoluminescence imaging and spectroscopy during microfluidic synthesis of cysteine-capped CdS quantum dot nanocrystals (CdS-Cys). Jun et al. (8) reported the UV/Vis spectroscopy coupled with microreactors for online process analysis of Au NPs produced in capillary reactor. Toyota et al. (9) also used online UV-vis spectrometer for analyzing CdSe Nanoparticles.

An inline measurement coupled with robust model-based control algorithm will be capable of synthesizing NPs with improved quality, consistency and throughput. Very few attempts have been made for complete automation of NPs synthesis. These reports are important as the complexities in automating nanoparticle synthesis with precise particle size and shape is far more complex than automating organic synthesis. In the first such attempt Krishanadasan et al. (10) demonstrated incorporation of an inline analytical detection method with an optimization algorithm. They observed significant improvement in the reaction optimization procedure by application of a microfluidic reactor as an autonomous "black-box" system for controlled synthesis. In this, two reaction parameters were controlled precisely while monitoring photoluminescence (PL) spectra to maximize the CdSe nanocrystal PL intensity. Toyota et al. (9) later reported a rapid screening system for CdSe quantum dots, using five parallel microreactors and inline fluorescence spectroscopy. This approach was effectively used for multiple reaction conditions, in order to determine and select of optimum conditions to obtain improved particle characteristics.

Machine learning has great potential and offers advantages in nanoparticle synthesis. Xueye and Honglin (11) reviewed studies using machine learning-assisted syntheses of nanoparticles. Self-driving micro-fluidic reactors integrated with machine learning have been used for the synthesis of quantum dots (Latif et al. 12), metal NPs (Berrada et al. 13) and lead halide perovskite nanocrystals (Epps et al. 14). In a fascinating work, Epps et al. 2020 (15)

developed a self-driving system named as Artificial chemist, which was capable of autonomous data generation, learning, and continuous on-demand manufacturing of solution-processed nanomaterials. This approach requires data from prior experiments. Same group developed a surrogate model which used data from over 1000 in-house conducted experiments of metal halide perovskite quantum dots synthesis.

While a significant body of literature exists on flow synthesis of nanomaterials, apart from these few studies no noticeable work has been reported for fully automated synthesis/production of nanomaterials. For achieving such a task, it is necessary to look at certain finer aspects of what can result into a deviation in the material specifications and to what extent. This becomes very crucial as it is almost impossible to develop separation at nanoscale to differentiate between particles within 5 nm deviation for any mean size. Such situations indicate that while flow synthesis helps achieve excellent control on size distribution, a process control algorithm that uses data from inline measurements to control the product properties is inevitable. Based on this data, the control algorithm will optimized the reaction condition using mathematical model and will drive the system towards a desired goal. Here we have made an attempt to couple an inline detection technique along with a developed model to predict the unsteady behavior of continuous NP's synthesis, which will sensitize the flow synthesis community at large on the complexity of inducing small unsteady features in the flow synthesis of nanomaterials.

Au NPs flow synthesis was used as a model system with an immiscible phase (heptane) that wets the wall and eliminates fouling of the reactor (11). Continuous organic phase forms a surrounding film around the aqueous droplets (12). Moreover, each formed aqueous phase droplet can be considered as a mixed reactor which moves along the tube length. Thus, a two-phase flow during NPs synthesis makes it analogous to a plug-flow reactor. Recently, Damilos et al. (16) developed a continuous manufacturing platform using flow reactor for the synthesis of aqueous colloidal gold nanoparticles (Au NPs). They also used two-phase flow system with heptane as the continuous phase which facilitated continuous syntheses for up to 2 h without wall deposition/fouling. In the current study we have used n-hexanol as a segmented fluid.

After this brief Introduction, this manuscript is organized as follows. In the next section we describe the experimental details and inline measurement system. Further we discuss the development of a mathematical model for the unsteady state plug flow reactor to predict the properties of Au NPs. The results and discussion section presents the estimation of kinetic parameters from batch experiments. The effect of various process parameters in flow synthesis is discussed followed by unsteady state experiments. Effect of step change in process conditions on the conversion of Au precursor and Au NPs size is discussed in detail. Further we compare the experimental results of unsteady state flow synthesis with those by simulation.

2. Experimental

2.1 Materials and methods

Hydrogen Tetrachloroaurate (III) Trihydrate ($HAuCl_4.3H_2O$, Alfa Aesar) **(HTCT)**, Trisodium citrate dihydrate **(TCD)**, 99% ($Na_3C_6H_5O_7.2H_2O$, Alfa Aesar) and Tris(hydroxylmethyl)-aminomethane **(THAM)**, 99% ($(HOCH_2)_3CNH_2$, Alfa Aesar). n-Hexanol, 99% ($CH_3(CH2)_4CH_2OH$, Loba Chemie) were used for synthesis of gold nanoparticles. De-ionised water was used for all the aqueous solutions throughout the experimental series.
The size distribution of nanoparticles and their mean size was measured using differential centrifugal sedimentation (DCS) (DC18000 Disc centrifuge, CPS Instruments, USA). Transmission electron microscopy (HR-TEM JEOL JEM F-200 electron microscope) of the samples was also performed to determine the morphology and also to verify particle size

distribution. Ocean optics spectrophotometer (USB2000+XR) was used for recording the online UV-Vis absorption spectra. Conversion of the Au precursor was measured by monitoring the temporal variation in the substrate concentration using 240FS-AA Atomic Absorption Spectrometer (Agilent Technologies). Solution pH was monitored using Thermo Scientific pH meter (Eutech pH 450).

2.2 Experimental setup

The flow synthesis of Au NP's was carried out in 2 m long, 1/16" Polytetrafluoroethylene (PTFE) tubing (1.58 mm outer diameter, 1.1 mm inner diameter) (VICI, USA). Ferrules, fittings and a micromixer (stainless steel 316) were used for all the required connections in the experimental set-up. Dual syringe pump (HO-SPLF-1, Holmarc Pvt. Ltd., India) was used for pumping the solution mixer at the required flow rate. The coiled reactor was dipped in an oil bath maintained at 90 °C in a stirring condition (450 rpm) placed on IKA RCT basic hot plate (Figure 1). The outlet stream was connected to a flow cell (quartz cuvette) of an inline U-Vis spectrometer to allow the synthesized AuNPs solution pass through the cuvette and record the position (λ_{SPR}) and the absorbance (A_{SPR}) data throughout the reaction. The AuNPs suspension leaving the flow cell was quenched in an ice bath to stop the reaction. Figure S1 shows the actual reaction setup.

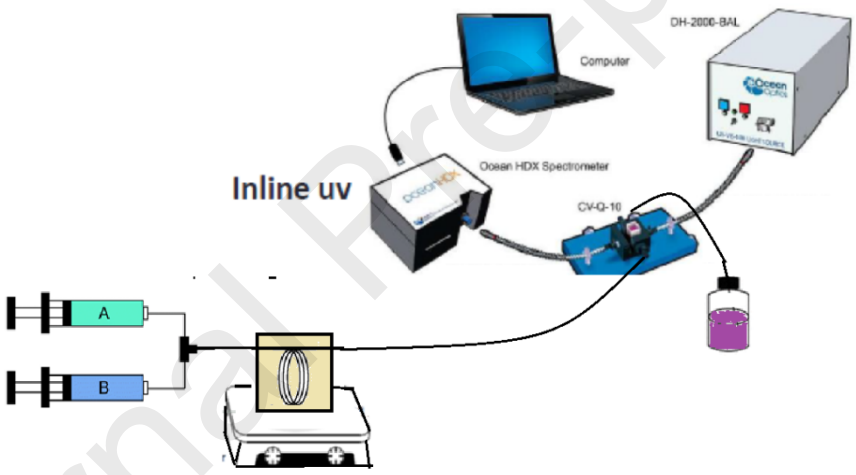

Figure 1: Schematic of the experimental setup for flow synthesis of AuNPs. Syringe pumps were used for dosing of Au precursor (A) and n-hexane (B).

3.1 Mathematical model for unsteady state plug flow synthesis of Au nanoparticles

In general, the plug flow reactors or even segmented flow reactors are considered to operate at steady state except for the start-up and shut-down times when the composition inside the reactor changes in space and time. In the present system under consideration, where we plan to study the response of the outlet product i.e. Au NPs (composition, particle size and shape) to certain operational perturbations, it is necessary to model the system in unsteady mode. The model should be capable of predicting the property monitored by inline measurements and thus would help comparing the transient situation at the outlet of the reactor. In this work, UV absorbance is monitored, which depends on mean particle size. The dependence of UV absorbance on NP size and number density for Au NP's is given as (14):

$$\lambda_{max} = 512 + 6.53\exp(0.0216\, d) \quad \text{.....(1)}$$

$$A_{450} = N \times 10^{-14} \times d^2\left[-0.295 + 1.36\, exp\left(-\left(\frac{d-96.8}{78.2}\right)^2\right)\right] \quad \text{.....(2)}$$

where, d is the diameter of Au NPs, N is the number of particle present per unit volume, λ_{max} is the peak wavelength of Au NPs sample, and A_{450} is the UV absorbance of Au NPs sample at wavelength of 450 nm. Thus, it becomes necessary to develop a model which can predict NP's size and number density. One of the widely used models for metallic NPs synthesis using reduction is the redox crystallisation (RC) model. The RC model predicts fractional conversion of precursor instead of particle size and number density, however, this approach can be modified to get the equations for particle size and number density.

3.1.1 RC Model

The RC model for the formation of Au NPs considers that the particle synthesis proceeds through two stages, i.e. reduction reaction and crystallization. and it can be represented by the following equations:

$$HAuCl_4 + Na_3C_6H_5O_7 \overset{K_c}{\leftrightarrow} Au_l^0 \quad \text{.....(3)}$$

$$Au_l^0 \overset{k_n}{\rightarrow} Au_s^0 \quad \text{.....(4)}$$

$$Au_l^0 + s^* \overset{k_g}{\rightarrow} Au_s^0 \quad \text{.....(5)}$$

It is assumed that the reduction of gold precursor ($HAuCl_4$) by reductants ($Na_3C_6H_5O_7$) is a reversible reaction in dynamic chemical equilibrium with an equilibrium constant K_c as shown in Eq. (3). Simultaneously, crystallization would occur whereby free soluble gold atoms in liquid phase (Au_l^0) get transformed into solid state (Au_s^0). Eq. (4) represents the typical phase transformation behaviours of Au_l^0 into Au_s^0 via nucleation, which is irreversible and the growth of nuclei via interaction between the surface active site (s^*) and (Au_l^0) is given in Eq. (5), which is also an irreversible phenomenon. Here k_n and k_g are the nucleation and crystal growth rate constants, respectively.

After considering the rate of individual reactions and some mathematical operations, the final form obtained for fractional conversion of Au precursor is given by:

$$X = 1 - \frac{k_1 + k_2}{k_2 + k_1 e^{(k_1 + k_2)t}} \quad \text{.....(6)}$$

Here k_1 and k_2 are modified kinetic parameters and based on Eq.(6), the RC model in terms of UV absorbance can be given as Eq. (7):

$$A_t = A_{max}\left(1 - \frac{k_1 + k_2}{k_2 + k_1 e^{(k_1 + k_2)t}}\right) \quad \text{.....(7)}$$

where A_t is the UV absorbance of Au NPs suspension at time *t* and A_{max} is the maximum UV absorbance of Au NPs suspension (i.e after complete conversion).

3.1.2 Modified form of RC Model:

As discussed earlier, the final form of RC model (Eq. 6) fails to predict the size and number density of NPs, and hence it needs to be modified to make it more useful for any design purpose. Although Eq. (7) gives UV absorbance with respect to time, this equation cannot be used for unsteady state as it involves A_{max} which varies with temperature, solution and agglomeration of nanoparticles. The modification is done to eliminate these constraints of the RC model. The modified RC model takes the following form:

$$[Au_l^0] = K_c\,[Na_3C_6H_5O_7][HAuCl_4] \quad \text{.....(8)}$$

$$\frac{d[Au_s^0]}{dt} = k_n[Au_l^0] + k_g s^*\,[Au_l^0] \quad \text{.....(9)}$$

Equation (9) comprises of two parts, i.e. nucleation and growth. Nucleation part is used to estimate the change in number of particles while growth part is used to calculate the change in average size of particles.

$$\frac{d[Au_s^0]}{dt} = \left(\frac{d[Au_s^0]}{dt}\right)_{nucleation} + \left(\frac{d[Au_s^0]}{dt}\right)_{growth} \quad \text{.....(10)}$$

$$\left(\frac{d[Au_s^0]}{dt}\right)_{nucleation} = k_n[Au_l^0] \quad \text{.....(11)}$$

$$\left(\frac{d[Au_s^0]}{dt}\right)_{growth} = k_g s^*\,[Au_l^0] \quad \text{.....(12)}$$

The rate of change in mass of NPs due to nucleation is given by

$$\left(\frac{d[Au_s^0]}{dt}\right)_{nucleation} = \frac{4}{3}\pi {r_n}^3 \rho \frac{dN}{dt} \quad \text{.....(13)}$$

Where $r_n$is the size of nuclei.

Thus we get

$$\frac{dN}{dt} = \propto \left(\frac{d[Au_s^0]}{dt}\right)_{nucleation} = \propto k_n[Au_l^0] \quad \text{.....(14)}$$

where $\propto = \frac{3}{4\pi {r_n}^3 \rho}$

Also the rate of change in mass of NP's due to growth is given by

$$\left(\frac{d[Au_s^0]}{dt}\right)_{growth} = \left(\frac{d[Au_s^0]}{dr}\right)_{growth} \times \left(\frac{dr}{dt}\right) \quad \text{.....(15)}$$

Considering average particle size as r_{avg} we have;

$$\left(\frac{d\left[Au_s^0\right]}{dr}\right)_{growth} = \frac{d}{dr}\left(\frac{4}{3}\pi\rho N {r_{avg}}^3\right) = 4\pi\rho N {r_{avg}}^2 = \beta N {r_{avg}}^2 \quad \text{.....(16)}$$

where $\beta = 4\pi\rho$

From equations (12), (15) and (16) we have;

$$\left(\frac{dr_{avg}}{dt}\right) = \frac{\beta k_g s^* \left[Au_l^0\right]}{N {r_{avg}}^2} \quad \text{.....(17)}$$

assuming the particles to be spherical in shape, the surface area of NP's is given by:

$$s^* = 4\pi N {r_{avg}}^2 \quad \text{.....(18)}$$

The amount of Au precursor remaining can be estimated by taking mass balance on gold concentration;

$$\left[Au^0\right] = \left[HAuCl_4\right] + \left[Au_l^0\right] + \left[Au_s^0\right] \quad \text{.....(19)}$$

and the fractional conversion is given by:

$$X = 1 - \frac{\left[HAuCl_4\right]}{\left[Au^0\right]} \quad \text{.....(20)}$$

The above set of algebraic and differential equations (Eqn. 14, 16, 17,18, 19 and 20) can be solved to get time evolution of average particle size and number of particles. These equations were solved in MATLAB using ODE45 solver and the parameter estimation (mainly the rate constants) was done by optimizing concentration profiles of Au precursor, Au NPs and average particle size. More details of optimization are given in SI.

3.1.3 Modified RC model for PFR:

The abovementioned equations are for batch operation. In order to use them for the unsteady flow synthesis, an unsteady state PFR model was developed and the final sets of equation are:

$$\frac{\partial[\dot{Au_s^0}]}{\partial z} = \frac{\pi D^2}{4}\left(k_n[\dot{Au_l^0}] + k_g s^* [\dot{Au_l^0}]\right) - \frac{\pi D^2 \partial[\dot{Au_s^0}]}{4 \quad \partial t} + \frac{\pi D^2 [\dot{Au_s^0}] \partial \dot{V}}{4\dot{V}^2 \quad \partial t} \quad \text{.....(21)}$$

$$\frac{\partial \dot{N}}{dz} = \frac{\propto \pi D^2}{4} k_n [\dot{Au_l^0}] - \frac{\pi D^2 \partial \dot{N}}{4 \quad \partial t} + \frac{\pi D^2 \dot{N} \partial \dot{V}}{4\dot{V}^2 \quad \partial t} \quad \text{.....(22)}$$

$$\left(\frac{\partial r_{avg}}{\partial z}\right) = \frac{\pi D^2 \beta k_g \dot{s^*} [\dot{Au_l^0}]}{4\dot{N} {r_{avg}}^2} - \frac{\pi D^2 \partial \dot{r_{avg}}}{4 \quad \partial t} + \frac{\pi D^2 \dot{r_{avg}} \partial \dot{V}}{4\dot{V}^2 \quad \partial t} \quad \text{.....(23)}$$

$$\dot{s^*}_Z = \left(4\pi \dot{N} \dot{{r_{avg}}^2}\right)_z \quad \text{..... (24)}$$

The above equations are for isothermal conditions. In order to consider temperature variations, Arrhenius type of equations are employed for reduction, nucleation and growth.

$$K_C = A_C e^{\frac{-E_C}{RT}} \quad \text{..... (25)}$$

$$k_n = A_n e^{\frac{-E_n}{RT}} \quad \text{..... (26)}$$

$$k_g = A_g e^{\frac{-E_g}{RT}} \quad \text{..... (27)}$$

The variation of temperature inside reactor due to change in bath (surrounding) temperature is obtained by incorporating heat balance equation:

$$\frac{dq}{dt} = -k\, A_T \frac{dT_r}{dR_t} \quad \text{..... (28),}$$

Which can also be given as

$$\frac{dq}{dt} = m.C_p \frac{dT}{dt} \quad \text{..... (29)}$$

where k is thermal conductivity of PTFE tube, A_T is the total surface area of tube, C_p is the specific heat capacity of fluid inside tube.

$\frac{dT_r}{dR_t}$ is the temperature gradient inside the tube which is established when the tube temperature is changed abruptly, while $\frac{dT}{dt}$ is the temporal change in temperature of fluid inside the tube. The specific heat capacity was taken based on the mass fraction of the fluids. Also as flow rate was very low, heat transfer due to convection was not considered.

These PDEs were converted into ODEs by discretizing the reactor into several small sections along the length. The obtained ODEs were solved in MATLAB platform using ODE45 solver. The relevant details viz. equations, boundary conditions, the initial condition are given in the Supporting Information. The kinetics estimated from batch synthesis were used to determine the conversion and particle size in flow synthesis. The obtained particle size and number density was utilized to get the simulated value of UV absorbance as per Eqn. (1) and (2).

4 Results and Discussions

4.1 Batch Synthesis

Citrate Reduction (reverse Turkevich) method that yields highly monodisperse AuNPs with size in the range of 10-20 nm was used for the synthesis of gold nanoparticles. In reverse synthesis method, the gold precursor HTCT was added to a heated stirring solution of TCD and THAM at desired temperature. The temperature of reaction mixture is held constant by immersing flask in an oil bath maintained at constant temperature. A significant improvement in the monodispersity, uniformity and size tunability with a change in pH of the Au nanoparticles has been observed by using THAM along with TCD in contrast to using only TCD. Several studies (17-22) have shown that small variations in the pH in citrate reduction method can alter the average particle size and is due to the different formation mechanisms of Au NPs at different pH conditions.

Several experiments were performed at different temperatures (85 ^{o}C, 90 ^{o}C, 95 ^{o}C and 100 ^{o}C) at 600 RPM to estimate the kinetic parameters. The initial concentration of HTCT in all of the experiment was 0.5 mM while the concentration of TCD was varied form 0.8 mM to 4 mM (TCD/HTCT ratio varied from 1.6 to 8). The pH of reaction mixture was observed to be between 4.5 to 6.5. Samples were taken periodically to monitor reaction conversion and AuNPs size. With an increase in reaction temperature to 100^{o}C more than 95% conversion was observed in a short time (Fig. 2) with the mean particle in the range of 25-35 nm. The particles

synthesized at lower temperature showed a considerable growth with the final particle size about 70±6 nm. The TEM micrographs depicted hexagonal shaped particles being formed (Figure 3).

4.2 Estimation of kinetics from the batch synthesis:

Experimental data at different temperatures, time, concentration and Au NP's size was utilized to estimate the kinetics of Au NP synthesis. Equations (14, 16, 17, 18, 19 and (20) were solved to estimate kinetic parameters by optimizing the time evolution of Au precursor concentration and average particle size. Parameters were estimated for Arrhenius form of equations (Eq. 25-27) so as to account for the temperature effects in transient experiments. The estimated parameters are given in Table 1. The values of pre-exponential factor and the activation energy indicated that while the nucleation is the fastest, it also needs sufficiently higher temperature to get activated. On the other hand, growth is a relatively slower phenomena with much lesser energy barrier.

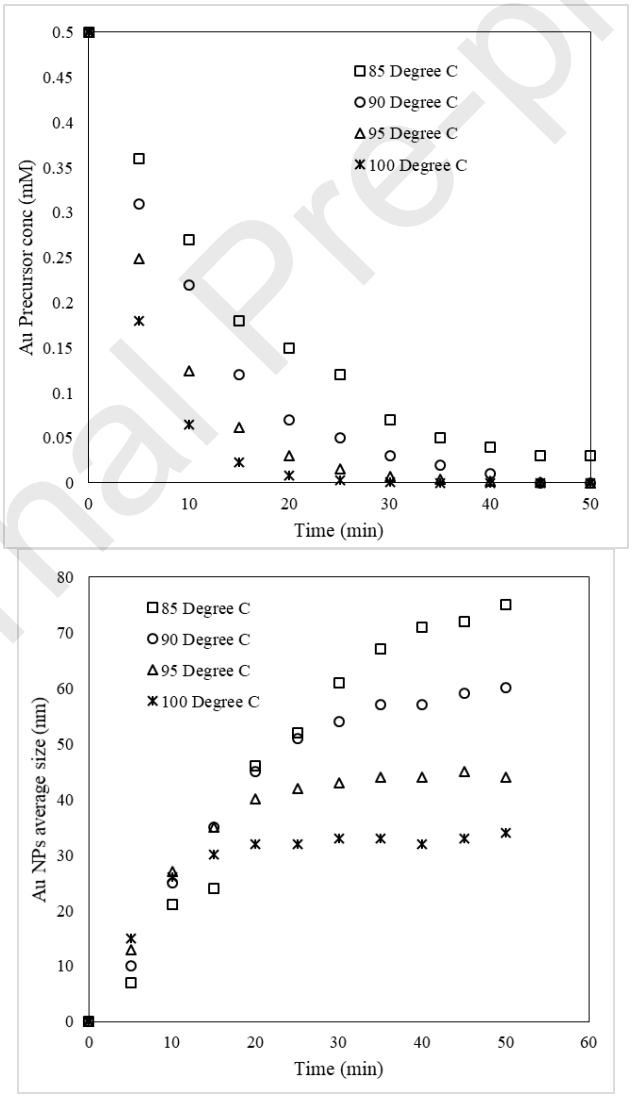

Figure 2. Experimental profile for (a) Au precursor concentration and (b) Au NPs average particle size for batch synthesis at varying temperatures, THAM = 4 mM and TCD = 1 mM.

Table 1. Au NP's synthesis kinetics using modified RC model.

Reaction step	Pre-exponential factor	Activation Energy (kJ/mole)
Reduction	9.884×10^{11}	87.73
Nucleation	1.095×10^{13}	92.20
Growth	4.811×10^{-8}	23.28

4.3 Flow synthesis

The process of reduction and its outcome (shapes and sizes) are intricately dependent on basic operational parameters, such as sequence of addition and efficiency of mixing of reagents. Hence maintaining reproducibility and consistent particle size from every batch experiment is a major challenge in this seemingly straightforward process, which further makes its scale-up more challenging. Continuous flow microreactors, by the virtue of their excellent control over reagent mixing in space and time within narrow channel networks, improved mass and heat transfer and enhanced reproducibility of the product properties produce AuNPs' in more reliable, reproducible and scalable ways. The batch kinetic data was utilized to determine the optimal operating conditions (residence time, flow rate) in flow mode of the reaction. Initial experiments on flow synthesis of gold nanoparticles without any segmenting fluid resulted in the particle deposition on the reactor walls (Fig S2). The deposition issue was overcame using an inert organic phase n-hexanol during the continuous reaction process. Both, the reactant aqueous phase and the organic phase are delivered at the same flow rate, which results in segmented flow that prevents the deposition of gold nanoparticles on the PTFE reactor walls during the course of reaction. The flow rate was calculated (0.15 ml/min) so as to have smaller Capillary number (Ca) to avoid clogging (23).

The likelihood of clogging can be assessed by clogging time, i.e. the time needed to reach clogging condition in a flow reactor. The clogging time depends on various parameters viz., particle density, particle concentration, fluid velocity, ratio of the particle settling velocity to superficial velocity, velocity profile in the reactor, physical properties of the fluid, etc. While smaller Ca can help avoid clogging, lower velocities can actually allow the particles to settle. It is reported in the literature that the use of hydrophobic microreactor and inert liquid dosing delays clogging and increases the clogging time (24). In the presence of inert liquid with non-wetting capillary wall, the deposition at the wall is minimal. In such case, the solids remain enclosed inside the dispersed phase (in this case aqueous phase) thus avoiding clogging. Hence although for some cases low capillary number may result in clogging, in current study clogging was not observed due to the presence of a dispersed phase. Segmented flow also ensures good mixing and narrow residence time distribution leading to reproducible gold nanoparticles (25). Typical TEM images of Au NPs synthesized in batch and flow are shown in Figure 3. It is quite evident that the product obtained in flow synthesis was similar in terms of size, shape and particle size distribution as that obtained in batch. Capillary number represents the relative effect of viscous forces vs. interfacial tension forces acting across an inter-face between two immiscible liquids. The change in the flow regime induced rapid

decrease in clogging time at higher Ca. The change in the flow regime induced rapid decrease in clogging time at higher Ca. It is reported that for liquid–liquid slug flow, for 0.0001 < Ca < 0.01, medium size slugs deform due to the Laplace pressure difference alongside the length of the slugs. Higher Ca corresponds to higher velocity in the capillary where the vortices

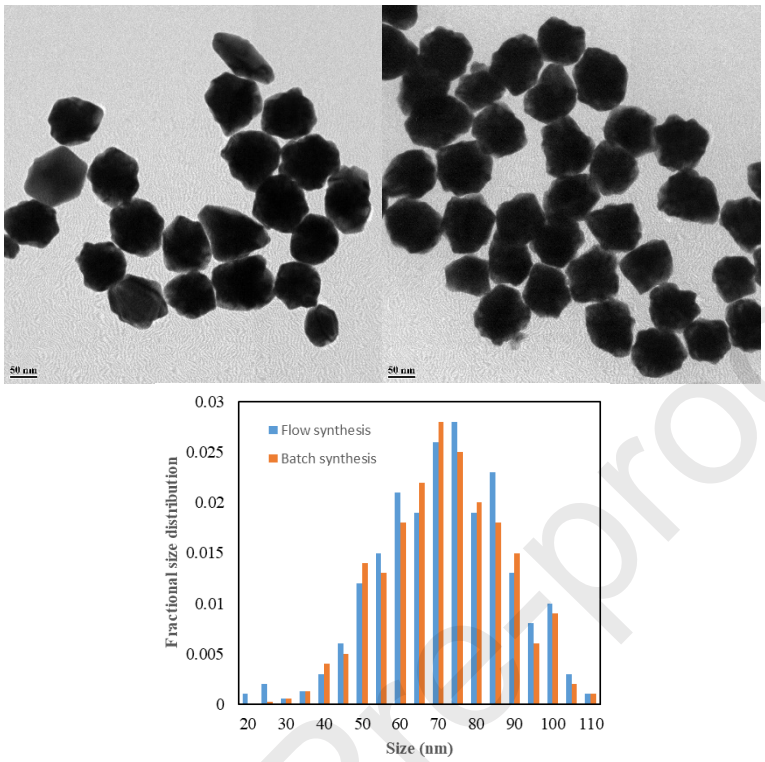

Figure 3: TEM images for Au NPs for (a) batch and (b) flow synthesis (c) Size distribution obtained from DCS. Temperature 85 ^{0}C, HTCT 0.5 mM, THAM = 4 mM and TCD = 1.2 mM, batch time 35 min and flow synthesis residence time 33 min.

become smaller in front and wider at the rear of the slug due to increase in shear forces and deformation of the slugs. This vigorous motion at the rear end of slug leads to reduction in the tendency of formation of the solid shells. In such a situation instead of shell formation, associative growth followed by cluster formation of precipitated salt particles takes place in the continuous aqueous phase leading to relatively faster clogging. In view of this, smaller Ca would help to avoid induction of rapid clogging in the capillaries.

4.4 Insights of the transient features of nanoparticle formation

To understand the response to perturbations in flow synthesis of Au NPs, several transient experiments in continuous flow mode were performed. These experiments were performed either by inducing a pulse change or a step change in temperature or flow rate of the reactant mixture. Details of the transient experiments performed are given in Table 2. Simulations were also performed to predict the average particle size and conversion after these perturbations and subsequently analyzing the transient behavior of process over wide range of conditions.

Table 2: HTCT, TCD and THAM concentrations, reactants and n-Hexanol streams flow rates and residence times in the 4ml reactor (*increase in the flow rate by 60% by short step change and **decrease in the flow rate by 60% by short step change)

Sr. No.	Concentrations			Flow rates		Residence time(min)	Temperature (^oC)
	HTCT (mM)	TCD (mM)	THAM (mM)	$V_{Reactant}$ (ml/min)	$V_{nHexanol}$ (ml/min)		
1	0.5	1.2	4	0.15	0.15	13.33	85 (↓ to RT)
2	0.5	1.2	4	0.15	0.15	13.33	90 (↓ to RT)
3*	0.5	1.2	4	0.24 (60%↑)	0.24	8.333	85
4**	0.5	1.2	4	0.06 (60%↓)	0.06	33.33	85

4.4.1 Transient temperature change:

The experiment 1 (Table 2, Entry 1) was carried out at 85 ^{0}C at a flow rate of 0.3 ml/min. The reaction was allowed to reach a steady state till 5 times residence time (= 5 x 13 min) and then was shifted to room temperature for a few time. The particles evolved during this course of fall in temperature were more polydispersed in nature as depicted by the particle images (Figure 4b and 4c). Subsequently, the temperature was increased to 85^{o}C to study the dynamic morphological behavior of AuNP's. Inline UV-Vis spectrophotometer continuously monitored the reaction dynamics as the product Au NPs solution passed through the flow cell. It was observed that the system attained steady state after 84 min and UV absorbance was restored to the value prior to first change in temperature. The particle size distribution was also found to be similar to those obtained before decrease in temperature. Similar results were also obtained for experiment performed at 90 ^{0}C, (Table 2, Entry 2).

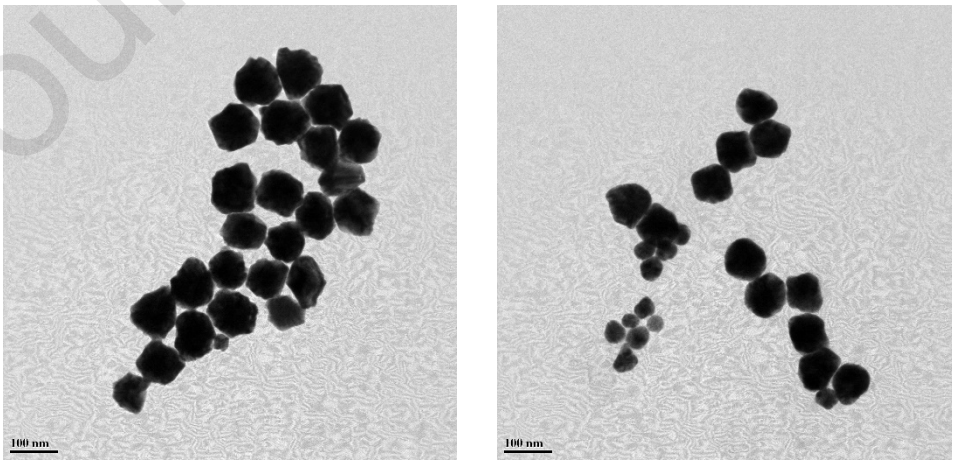

(a) (b)

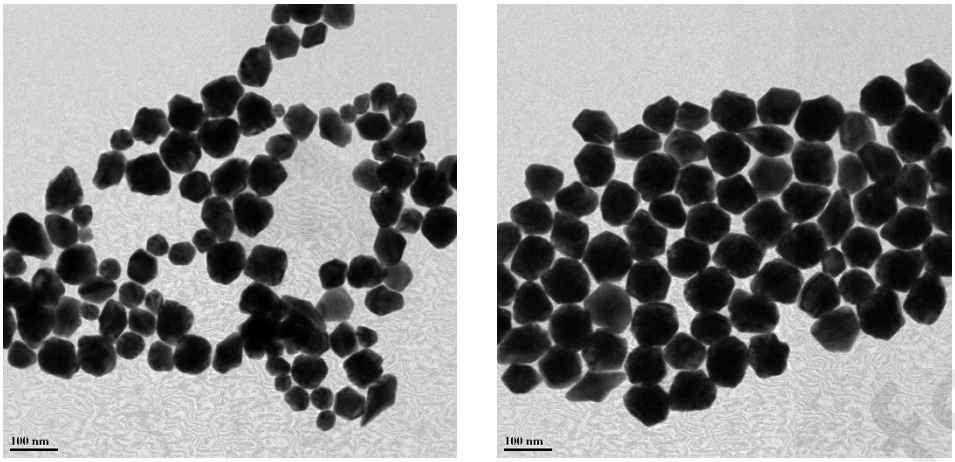

(c) (d)

Figure 4: TEM micrographs for AuNPs collected after regular intervals of time during the progression of reaction with transient change from 85 ^{0}C to 35 ^{0}C: (a) 40 min, (b) 60 min, (c) 80 min and (d) 100 min.

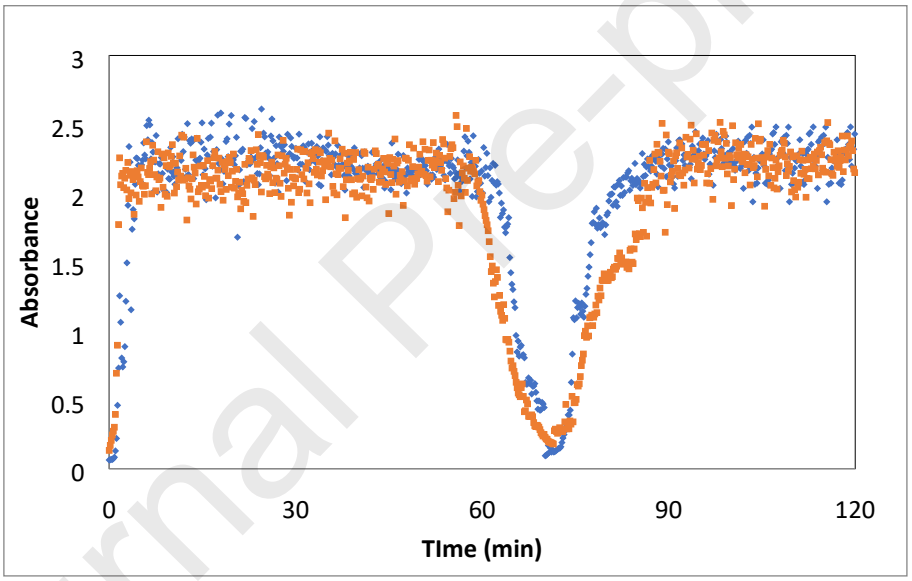

Figure 5: Comparison of experimental UV absorbance at 450 nm for the transient experiment of pulse change in temperature at (i) ● [90 ^{0}C] and (ii) ● [85 ^{0}C] for HTCT = 0.5 mM, TCD = 1.2 mM and THAM = 4 mM.

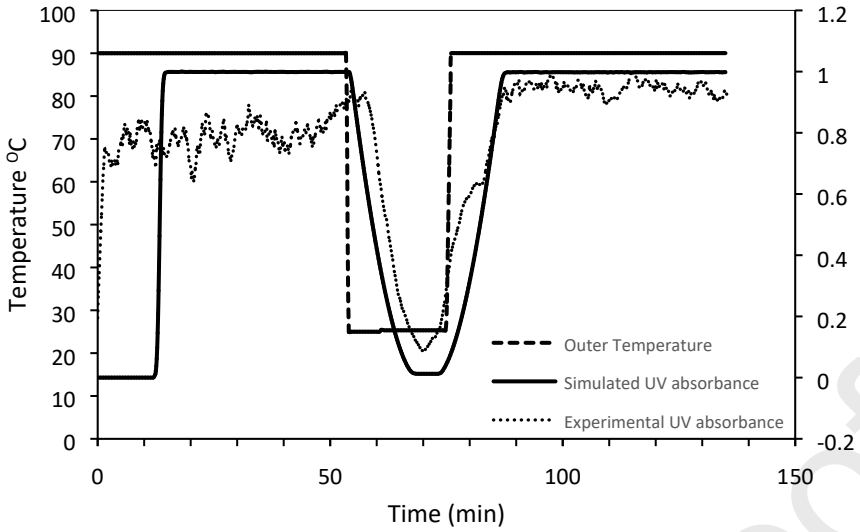

Figure 6: Experimental vs simulated normalized UV absorbance profile at 450 nm for transient experiment at 85 ^{0}C and reduction to room temperature.

Typical nature of response of flow synthesis to these perturbations can be assessed based on inline UV data. Figure 5 shows the comparison of inline UV absorbance data with time at two different temperatures of 85 ^{0}C and 90 ^{0}C, which shows almost similar nature of response at both temperatures. Simulations were carried out for these two transient experiments to predict UV absorbance as per Equation (2). A comparison between experimental and theoretical UV absorbance is shown in Figure 6. The simulated profile showed trends similar to the actual experimental data with an over estimation by 6.67% than the actual value, which is not a very large deviation. This implied that the modified RC model is able to capture the dynamic behavior of system correctly but only in terms of trend and transient response. Difference was observed in terms of exact magnitude of the UV absorbance, i.e. concentration of particles.

Several simulations were also performed for transient temperature change; viz. (i) Case 1: flow synthesis of Au NP at 90 ^{0}C for 54 min followed by a step change in the bath temperature to 25 ^{0}C for 20 min followed by immersing the reactor again in oil bath maintained at 90^{0}C. In this case, thermal conductivity effect was not considered. (ii) Case 2: Same as Case 1 except that the heat transfer effect was considered. (iii) Case 3: Pulse change in temperature after 54 min by reducing temperature from 90 ^{0}C to 25 ^{0}C for only 0.1 minute followed by immersing the reactor again in oil bath maintained at 90 ^{0}C. (iv) Case 4: feed A and B were separately heated before mixing and bath temperature was give step change from 90 ^{0}C to 25 ^{0}C for 20 min. Figure 7 shows the results for various cases of transient temperature simulations.

When the thermal conductivity of the tube wall is not considered in the model, an immediate fall in Au NPs size is observed when compared with the cases where thermal conductivity effects were taken into account. Although the difference was small, we can conclude that considering thermal resistances actually delays the effect of disturbance. Since incorporation of heat transfer equations (for segmented flow in a PTFE tube) gave temperature profile close to the actual temperature profile, in all subsequent simulations involving temperature change, heat transfer equations were considered to have a more accurate depiction of the outlet observations. As temperature is kept constant at 25^{0}C for some time in both, Case 1 and Case 2, the outlet concentration of Au precursor attains the same value as that at inlet

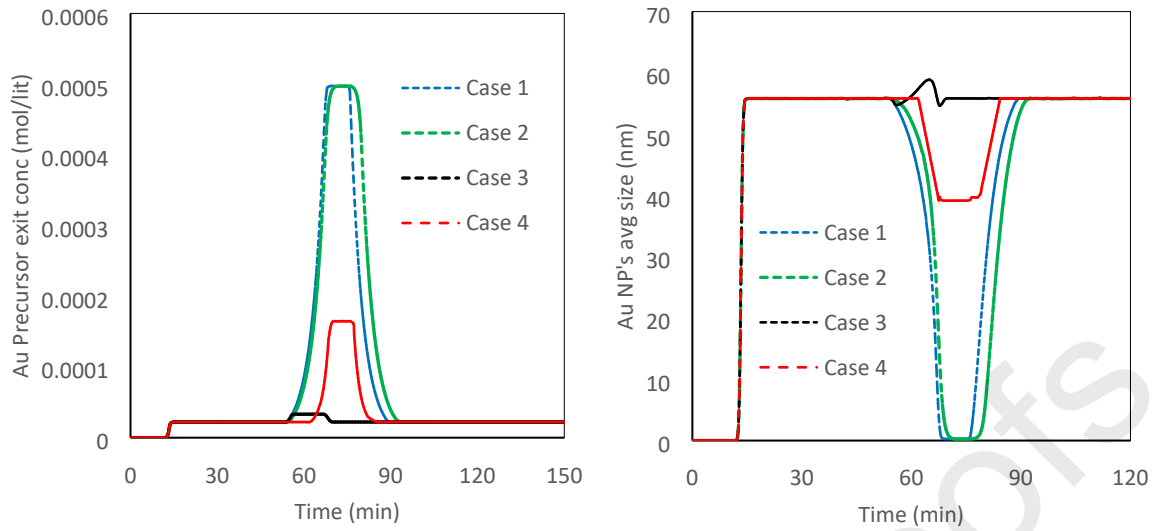

Figure 7: Simulation results for transient temperature cases. (Left) Transient variation in the exit concentration of $HAuCl_4$ precursor, (Right) Transient variation in the average Au NP's size. (HTCT = 0.5mM, TCD = 1.2mM and THAM = 4 mM, Residence time = 13.33 min.)

indicating almost negligible conversion. The same was evident from the average Au NPs size which falls to zero. For pulse change in temperature, slight increase in Au NPs size is observed before it reverts to the original value. This increase in the particle size showed that none of the slugs of Au precursor attains the minimum temperature of 25 ^{0}C in the time period of pulse change (0.1 min). In Case 3, most of the slugs are at quite higher temperature but lower than 90 ^{0}C. Reduction in the temperature over a short time reduces the nucleation rate and later enhances the growth rate leading to slightly bigger size Au NP before returning to a steady value as before. Thus, although for the short time period, the conversion is lower, corresponding particle sizes at the outlet are larger. Importantly, the entire duration for which the effect of a pulse change of 0.1 minute is seen at the reactor outlet is almost equal to residence time, which is quite significant. Also for case 4, in which feed A and B were separately heated before mixing and bath temperature was given a step change, the change in outlet concentration was delayed as compared to case 1 to 3 in which feed were not preheated. This is because as feed is preheated, actual drop in temperature of reaction mass will not be immediate. This will largely depend on heat transfer coefficient which is very low for current system due to laminar flow inside reactor. The final temperature obtained inside the reactor in case 4 is higher than that obtained in case 1 and case 2. Due to this conversion is higher and hence Au precursor exit concentration is lower in case 4. When experiments were performed at these corresponding conditions, the observations were seen to be correct and a slight red shift in the UV-vis spectra was observed for a very short time. With these observations, it was further necessary to assess the effect of other transient effects on the particle properties.

4.4.2 Transient flow rate change:

In order to study the effect of change in flow rate of reactants during reaction, three different cases were simulated. These cases are: (i) Case 5- Increasing flow rate by 60% after 54 min (i.e. after 4 residence times) for 1 min followed by reverting to the original value. (ii) Case 6: repeat Case 4 by keeping the higher flow rate only for 0.1 min. and (iii) Case 7: Same as case

6 but the only difference is change in flow rate was 100%. Figure 8 shows the results for various cases of transient flow rate experiments.

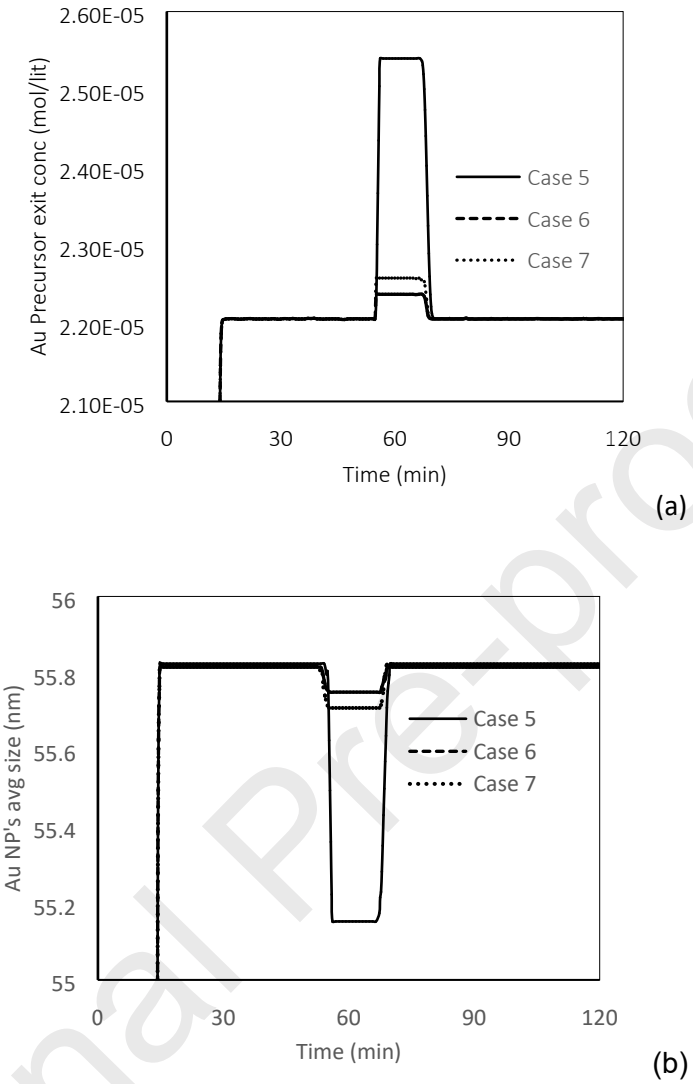

Figure 8: Simulation results for transient flow rate cases. (a) Simulated profile for HTCT precursor exit concentration. (b) Simulated profile for average Au NPs size. (HTCT = 0.5mM, TCD = 1.2mM and THAM = 4 mM, Initial residence time = 13.33 min, residence time during perturbation: Case 4 = 8.33 min, case 5 = 8.33 min and case 6 = 6.67 min.)

Variations in the flow rate were seen to affect the reaction progress only marginally even for 100% increase. Although the effect of pulse change by 60% for 1 min on Au precursor exit concentration is observed to be higher, effect on Au NPs size is negligible. On the other hand, pulse change of even smaller duration 0.1min does not affect Au precursor outlet concentration significantly. In any case, the effects of such a change were significant in terms of their time foot print as even for a change for 0.1 minute, the actual time needed to reach the steady state was more than one residence time.

Several simulations were carried out to understand the time needed for system to reach steady state for different time steps for which changes were made. A linear relationship was observed between them for all the three variables (Figure 9). However, the time required for attaining

the steady state was highest for temperature change as compared to others. This is quite obvious as temperature change affects every slug moving in the reactor and hence it affects conversion even in slugs which are about to leave the reactor. On the other hand, recovery to steady state was fastest in the case of change in inlet concentration. Since dispersion effects were not considered, slugs already present in the reactor were not affected by any change in inlet concentrations. Thus, one would expect the time required for attaining steady state would be equal to the total time taken between initiation of change and the time when the system attained its original conditions.

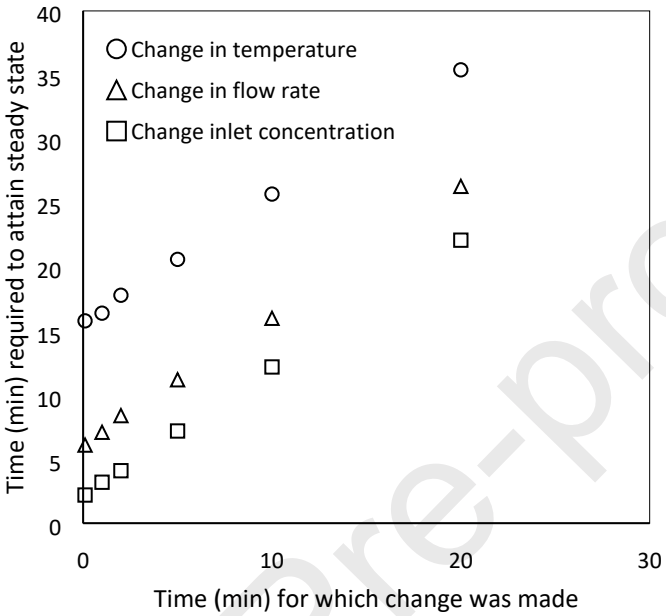

Figure 9 . Time needed for system to reach steady state vs. time for which condition was changed. (HTCT = 0.5mM, TCD = 1.2mM and THAM = 4 mM, Residence time = 13.33 min) (Change in conditions is achieved gradually in 1 min for all cases).

It is also important to know how quickly changes are induced in the system and as a result how system behaves. Figure 10 shows the response of Au NPs synthesis to a short-lived change (1 min), but the rate of change was varied. Similar to the previous case, it was observed that the change in temperature causes significant disturbance in the system and it required long time recover. Even for a deviation in the system for as small as 1.2 min from constant temperature (0.1 min cooling + 1 min steady temperature + 0.1 min heating to attain original temperature), the system took almost 15 min to regain its original steady state. Although in this case, scale of temperature change was higher (from 90 ^{0}C to 25 ^{0}C and again back to 90 ^{0}C), we can say that even a short-lived and rapid change in temperature can substantially affect the quality of Au NPs.

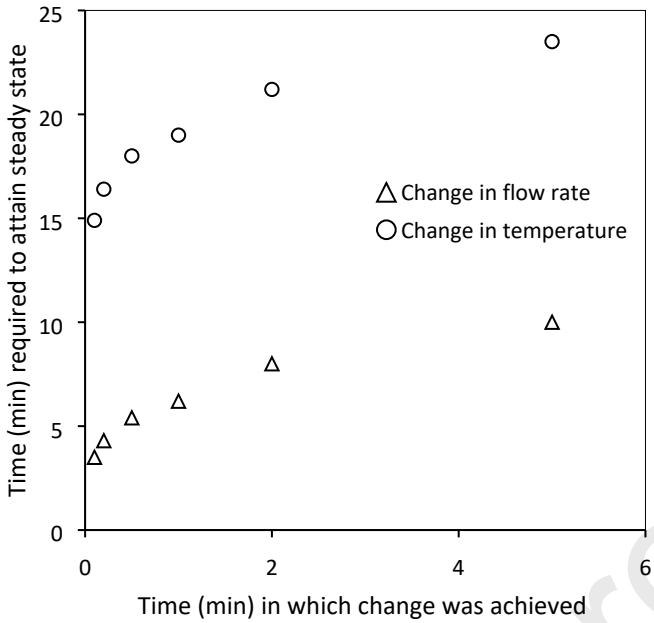

Figure 10. Time needed for system to reach steady state vs. time in which change was achieved. (HTCT = 0.5mM, TCD = 1.2mM and THAM = 4 mM, Residence time = 13.33 min) (Change in conditions is for 1 min for all cases.).

4.4.3 Perturbation in the inlet concentration:

In order to study the effect of change in the inlet concentration, simulations were carried out for different conditions for transient change in concentration with both pulse and step changes once the system reaches steady state. These are given as Case 8-10, where in Case-8, after 60 minutes, the inlet Au precursor concentration was decreased by 40% and kept constant subsequently, while in Case 9 it was increased by 40% and kept constant subsequently. In Case 10, a pulse change of concentration was done by reducing concentration by 40% from 0.5 mM to 0.3 mM for only 1 minute after running the reactor for 60 min at steady state. The outlet concentration as well as particle size were monitored to understand the actual time needed to reach a subsequent steady state. Figure 11 shows the results for various cases of transient inlet concentration experiments.

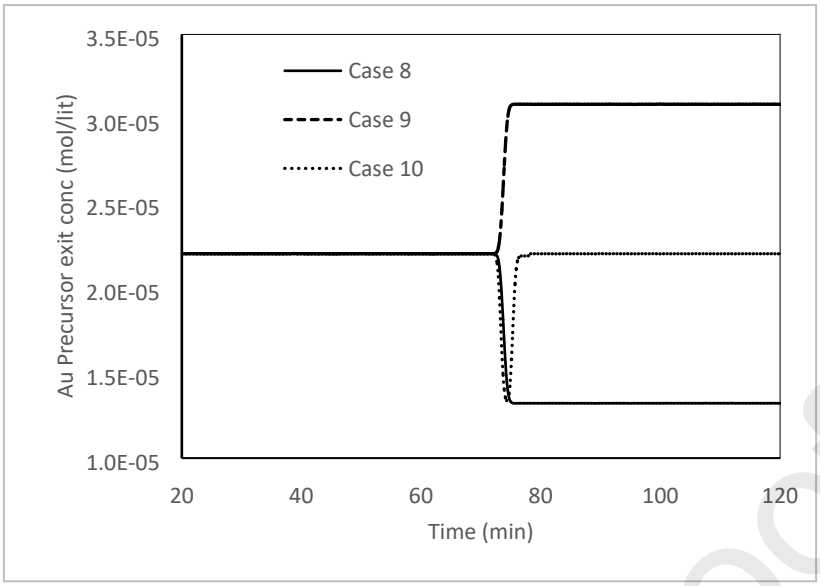

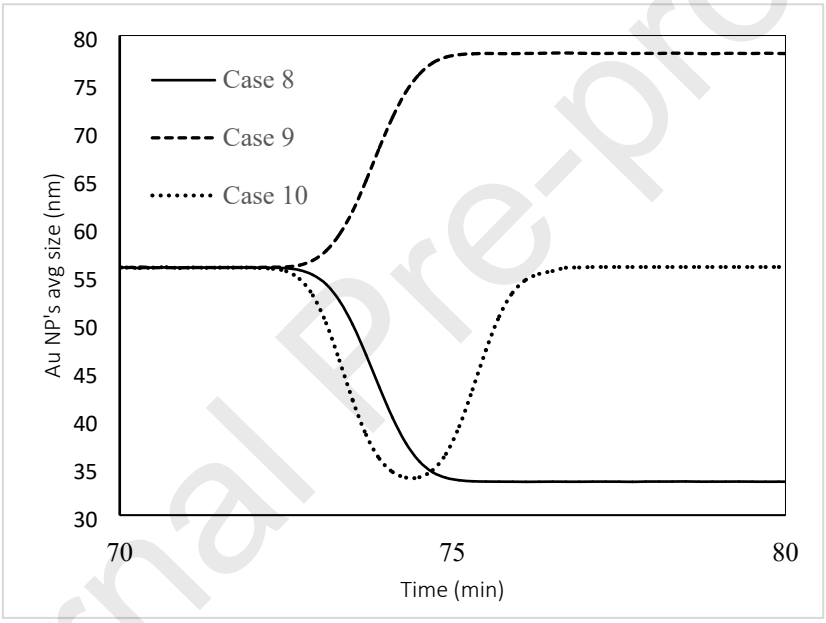

(a) (b)

Figure 11: Simulation results for transient inlet concentration cases. (a) Simulated profile for HTCT precursor exit concentration. (b) Simulated profile for average Au NP's size. (TCD = 1.2mM and THAM = 4 mM, Residence time = 13.33 min, Initial HTCT concentration = 0.5mM, HTCT concentration during perturbation: Case 7 = 0.3mM, Case 8 = 0.7mM and case 9 = 0.3 mM)

The effect of transient change in inlet concentration is quite predictable. The change in inlet concentration is reflected after a delay of residence time. Moreover, it does not affect the reaction mixture which is already present in flow reactor prior to change and hence a gradual shift to another steady state is observed. This is also observed for all the cases where sudden change in exit concentration of Au precursor is observed at around 73 min. The pulse change made for 1 minute was seen to remain effective for almost 4 minutes and the particle size varied over 34 - 55 nm. This implies that continuously pulsating system will always give continuous variation in the particle size and hence would result in a wide size distribution and

the rate of pulsation will decide the nature of distribution (i.e. Gaussian or bimodal or multimodal). In view of this, it is necessary to maintain fixed concentration as well as fixed flow rate of the substrates, which is the key requirement of ensuring the desired nucleation as well as growth rates. This also implies that using the right kind of pumping system with zero pulsation or variation is an essential requirement for flow synthesis of nanoparticles, even in segmented flow regime.

Further, the effects of these changes are seen to be a strong function of the duration of variation as well as the rate of variation. Thus, making a flow synthesis faster to reduce the foot print of a set-up is also more prone for showing pronounced effects of pulsation or variation in the conditions. Overall, the effect of change in temperature in flow synthesis of Au NPs is found to be the most profound, if gets coupled with concentration change, the overall result will be quite different and would last for a significantly longer duration than that for which change is made.

5 Conclusions

Transient effects of perturbations in flow synthesis of nanoparticles on the particle sizeis presented for the first time. The flow synthesis of Au NPs was taken as a model system. An inline UV-Vis spectrometer was used for recording the variation in the position of the highest absorbance (λ_SPR) and the intensity of absorbance (A_SPR) data before, during and after a perturbation was set. Batch experiments were carried out by the citrate reduction method to estimate the kinetic parameters in the Arrhenius form so as to account for the temperature effects in transient experiments for reduction reaction, nucleation and growth phase. Segmented flow was used for avoiding wall deposition.. The perturbations in flow synthesis were induced either by giving pulse change or by giving a step change in the reactor temperature or flow rate of the reactant mixture or concentration of the reactants when the reactor was in a steady state.

A Modified Redox crystallisation (RC) model comprising of nucleation and growth components incorporated in the design equation for non-isothermal PFR was used to calculate the temporal evolution of average particle size and number of particles. Simulated UV-vis absorbance that corresponds to the concentration of gold nanoparticles in the solution showed excellent match with the experimental data, which implied that the modified RC model is able to capture the dynamic behavior of the system correctly. Upon changing the flow rate of reactants, the simulated profile showed only marginal effect on the reaction progress even for 100% increase, however the effects of such a change were significant in terms of their time foot print as for a change for 0.1 minute, the actual time needed to reach the steady state was more than 10 times the perturbation time. The time needed for the system to reach steady state for different time steps for which the flow rate was changed showed a linear relationship. However, the time required for attaining the steady state was highest for temperature change as compared to other parameters.

Quick change in the inlet concentration was seen to be reflected in terms of a gradual shift to another steady state and with a significant change in the particle size. This observation is critical as a continuously pulsating system will always give continuous variation in the particle size and hence would result in a wide size distribution. The time required for the system to regain its steady state was observed to depend on: (i) variable which is changed, (ii) how quickly the change is made and (iii) duration for which the change is made. With the efforts towards moving into automation and high throughput screening/synthesis of nanomaterials in continuous flow mode, the results from this work clearly indicate that it is necessary to ensure that deviations from the desired steady state operations are avoided or a feedback control system and a transient waste collection system need to be implemented.

Acknowledgements

The authors thank the DST-UKIERI 2017-18 (contract IND/CONT/G/17-18/47) scheme for funding this work. AHB thanks DST-SERB for National postdoc fellowship (File no. PDF/2018/002599).

References:

1. Mahmoud, Mahmoud A., Daniel O'Neil, and Mostafa A. El-Sayed. "Hollow and solid metallic nanoparticles in sensing and in nanocatalysis." *Chemistry of Materials* 26.1 (2014): 44-58.
2. Patil, Prathamesh, et al. "Inkjet printing of silver nanowires on flexible surfaces and methodologies to improve the conductivity and stability of the printed patterns." *Nanoscale Advances* 3.1 (2021): 240-248.
3. Wilson, Robert. "The use of gold nanoparticles in diagnostics and detection." *Chemical Society Reviews* 37.9 (2008): 2028-2045.
4. Chomoucka, Jana, et al. "Magnetic nanoparticles and targeted drug delivering." *Pharmacological research* 62.2 (2010): 144-149.
5. Sebastian, V. et al. "Perspective Article: Flow Synthesis of Functional Materials", J. Flow Chem. 7, (2017): 96–105
6. Yue, Jun, Jaap C. Schouten, and T. Alexander Nijhuis. "Integration of microreactors with spectroscopic detection for online reaction monitoring and catalyst characterization." *Industrial & engineering chemistry research* 51.45 (2012): 14583-14609.
7. Sounart, T. L., et al. "Spatially-resolved analysis of nanoparticle nucleation and growth in a microfluidic reactor." Lab on a Chip 7.7 (2007): 908-915.
8. Yue, Jun, et al. "Microreactors with integrated UV/Vis spectroscopic detection for online process analysis under segmented flow." *Lab on a Chip* 13.24 (2013): 4855-4863.
9. Toyota, Ayumi, et al. "Combinatorial synthesis of CdSe nanoparticles using microreactors." *The Journal of Physical Chemistry C* 114.17 (2010): 7527-7534.
10. Krishnadasan, S., et al. "On-line analysis of CdSe nanoparticle formation in a continuous flow chip-based microreactor." Journal of Materials Chemistry 14.17 (2004): 2655-2660.
11. Chen, X. and Honglin Lv. "Intelligent control of nanoparticle synthesis on microfluidic chips with machine learning." *NPG Asia Materials* 14.1 (2022): 69.
12. Abdel-Latif, K. et al.. Self-driven multistep quantum dot synthesis enabled by autonomous robotic experimentation in flow. *Advanced Intelligent Systems*, *3*(2), (2021), 2000245.
13. Epps, R. W., Volk, A. A., Reyes, K. G., & Abolhasani, M. (2021). Accelerated AI development for autonomous materials synthesis in flow. Chemical Science, 12(17), 6025-6036.
14. Mekki-Berrada, F. et al. Two-step machine learning enables optimized nanoparticle synthesis. *npj Computational Materials*, *7*(1), (2021) 55.
15. Epps, R. W., et al. Artificial chemist: an autonomous quantum dot synthesis bot. Advanced Materials, 32(30), (2020). 2001626.
16. Damilo, Spyridon, et al. "Continuous citrate-capped gold nanoparticle synthesis in a two-phase flow reactor." *Journal of Flow Chemistry* (2021): 1-15.
17. Mello, John de, and Andrew de Mello. "FocusMicroscale reactors: nanoscale products." *Lab on a Chip* 4.2 (2004): 11N-15N.

18. Damilos, Spyridon, et al. "Continuous citrate-capped gold nanoparticle synthesis in a two-phase flow reactor." *Journal of Flow Chemistry* 11.3 (2021): 553-567.
19. Haiss,Wolfgang, et al. "Determination of size and concentration of gold nanoparticles from UV− Vis spectra." *Analytical chemistry* 79.11 (2007): 4215-4221.
20. Kumar, Sanjeev, et al. "Modeling of formation of gold nanoparticles by citrate method." Industrial & Engineering Chemistry Research 46.10 (2007): 3128-3136.
21. Pong, Boon-Kin, et al. "New insights on the nanoparticle growth mechanism in the citrate reduction of gold (III) salt: formation of the Au nanowire intermediate and its nonlinear optical properties." The Journal of Physical Chemistry C 111.17 (2007): 6281-6287.
22. Li, Chunfang, et al. "Facile synthesis of concentrated gold nanoparticles with low size-distribution in water: temperature and pH controls." *Nanoscale research letters* 6.1 (2011): 1-10.
23. Pal, S. and A. A. Kulkarni. "Interfacial precipitation and clogging in straight capillaries." *Chemical Engineering Science* 153 (2016): 344-353.
24. Pal, Sayan, and Amol A. Kulkarni. "Quantitative comparison of strategies to delay clogging in straight capillaries." Chemical Engineering Science 199 (2019): 88-99.
25. Günther, Axel, et al. "Transport and reaction in microscale segmented gas–liquid flow." *Lab on a Chip* 4.4 (2004): 278-286.

Declaration of interests

☒ The authors declare that they have no known competing financial interests or personal relationships that could have appeared to influence the work reported in this paper.

☐The authors declare the following financial interests/personal relationships which may be considered as potential competing interests:

I am signing this as the corresponding author on behalf of all the authors.

Dr. Amol A. Kulkarni

Scientist, Chemical Engineering Division

National Chemical Laboratory

Pune – 411 008, India

26.

Highlights

- This is the first ever report on response to transient perturbations in flow synthesis of Au NP.
- Experimentally obtained kinetics were used for developing mathematical model for predicting dynamics.
- Inline UV-vis spectra helped monitor the real time response to perturbations in temperature and flow rate.
- A small change in process variables for short duration needed significantly long time to reach a steady new particle size.
- The effect of temperature variation was seen to have the slowest effect on reaching a new steady state.

27.